Available online at www.sciencedirect.com
ScienceDirect
Catalysis Today 120 (2007) 317–323
CATALYSIS TODAY
www.elsevier.com/locate/cattod

Quantitative structure–uptake relationship of metal-organic frameworks as hydrogen storage material

Daejin Kim [a], Junhyoung Kim [a], Dong Hyun Jung [a], Tae Bum Lee [a], Sang Beom Choi [b], Ji Hye Yoon [b], Jaheon Kim [b], Kihang Choi [c], Seung-Hoon Choi [a,*]

[a] *Insilicotech Co. Ltd., A-1101 Kolontripolis, 210, Geumgok-Dong, Bundang-Gu, Seongnam-Shi 463-943, Republic of Korea*
[b] *Department of Chemistry, Soongsil University, 1-1, Sangdo-5Dong, Dongjak-Gu, Seoul 156-743, Republic of Korea*
[c] *Department of Chemistry, Korea University, 1, Anam-dong 5-Ga, Seongbuk-Gu, Seoul 136-701, Republic of Korea*

Available online 13 November 2006

Abstract

We have investigated the relationship between the molecular structures of metal-organic frameworks (MOFs) and their hydrogen uptake capabilities. Quantitative structure–property analysis was used to find out MOF structural factors important for hydrogen adsorption. To determine the quantitative interaction strength between hydrogen molecules and MOFs, the iso-value surface area of electrostatic potential was developed as a new descriptor. Quantitative analysis of structurally similar MOFs showed that the functionalization of aromatic organic linkers could induce noticeable polarization effect on the framework surface. We also found that the topology of MOFs plays an important role in determining the amount of ultimate hydrogen uptake. Through this quantitative structure–uptake relationship analysis, structural descriptors for the prediction of MOF hydrogen sorption capacity have been identified.

Keywords: Hydrogen adsorption; QSPR; Metal-organic frameworks; MOFs; Polar surface area

1. Introduction

Metal-organic frameworks (MOFs) are microporous crystalline solids that consist of three-dimensional networks of inorganic and organic building units. Unlike zeolites and many other porous networks, MOFs have the potentials to exhibit properties such as chirality, framework interpenetration, or framework flexibility [1]. Because of these unique and interesting properties, MOFs have been explored for various applications including the efficient storage of volatile fuels like hydrogen. Recently, Yaghi and co-workers reported that a series of isoreticular MOFs (IRMOFs), $Zn_4O(L)$ (L = linear aromatic dicarboxylates), have reversible hydrogen storage capacities [2]. Inelastic neutron scattering (INS) experiments showed that hydrogen adsorption occurs primarily on Zn metals and additional interaction sites can be provided by organic linkers. Thus, both metal and organic units play important roles in hydrogen uptakes, and several strategies for optimizing the building units have been suggested [3].

To design MOFs with high hydrogen-storage capacities, it is important to understand how structural changes affect hydrogen uptake properties. This structure–uptake relationship, however, seems very specific for each system studied [4–7]. In addition, INS [2] and X-ray diffraction [8] data, which provide valuable information about the interaction between the frameworks and hydrogen molecules adsorbed, are only available for a handful of MOFs. Moreover, the correlation between the structural features of MOFs, such as the density of the aromatic rings per formula unit, framework interpenetration, surface area, the sort of metal ions, organic functional groups, and the presence of the open metal sites [9–14], makes it more difficult to analyze the structure–uptake relationships.

Previous theoretical studies suggested that there might be several factors affecting the hydrogen adsorption capability of MOFs [15–18]. Quantum mechanical and statistical simulation analysis showed that the balance between surface area and porosity is critical for the efficient physisorption of hydrogen molecules. The electrostatic potential of MOF was suggested to be another important factor because the binding energy of

* Corresponding author. Tel.: +82 31 728 0443; fax: +82 31 728 0444.
E-mail address: shchoi@insilicotech.co.kr (S.-H. Choi).

0920-5861/$ – see front matter
doi:10.1016/j.cattod.2006.09.029

hydrogen is presumably related with the electron density of the framework. Understanding the relationship between these structural factors and hydrogen uptake in a more quantitative way would be helpful for the development of MOFs as efficient hydrogen storage materials.

In this study, we introduced quantitative structure–property relationship (QSPR) analysis to predict the extent of hydrogen adsorption depending on the molecular structure of MOFs. To find out the key structural elements for efficient hydrogen uptake, QSPR methods were used to formulate the functional relationship between the target property and the molecular descriptors. During QSPR analysis, molecular descriptors are selected to represent molecular structures quantitatively and the correlation is generally characterized by using regression analysis, genetic algorithm [19], recursive partitioning [20–22], and artificial neural network [23]. We developed the iso-value surface area of electrostatic potential as a new descriptor which can represent the molecular field of MOF pores. This and other two- and three-dimensional descriptors were used for the multiple linear regression analysis and the classification of MOFs with recursive partitioning. As a result, we could characterize the relationship between hydrogen uptake and the molecular structure of MOFs.

2. Computational details

2.1. Analyzed MOF structures and collection of hydrogen uptake data

Among the previously studied MOFs with known crystal structures and hydrogen uptake properties, we selected five IRMOFs for model building and other studies (Table 1). We also synthesized five additional MOFs and characterized their hydrogen sorption properties. IRMOF-3β has the same framework formula and similar structure as IRMOF-3 ($Zn_4O(NH_2BDC)_3$), (BDC = benzene dicarboxylate) but has NH_2 groups at symmetric positions on the organic linkers. The framework formulas of other MOFs are $Zn_7O_2(NO_2BDC)_5$ for NitroMOF, Zn_3(2,6-NDC)$_3$(dabco) (NDC = naphthalene dicarboxylate, dabco = triethylene diamine) for Zn26NDC_dabco, Zn(2,7-NDC) for Zn27NDC_block, and $Zn_4O(BTB)_2$ (BTB = benzene-1,3,5-tribenzoate) for ZnBTBd. ZnBTBd has same framework building blocks as MOF-177, but forms different framework net with double interpenetration. Among the 10 MOFs studied, IRMOF-1, -3, -3β, and -8 have almost the same framework topology of a simple cubic net, but the organic linkers of the four MOFs are different from each other with respect to the position and/or the sort of substituents. Other MOFs with very different framework topology were selected to examine the influence of topological change.

All hydrogen sorption data compared were collected under the same experimental conditions (77 K, 1 atm) and the data was fitted against an ideal isotherm equation to determine the ultimate hydrogen uptake value at infinite pressure. Langmuir–Freundlich (LF) equation [24] has been used successfully to explain gas adsorption properties of porous materials such as MOFs, Prussian Blue derivatives, and activated carbon [25]. Saturated amounts of hydrogen in MOFs were estimated by fitting the adsorption data against LF equation (Eq. (1)), where B is the amount of hydrogen adsorbed at 77 K and partial pressure P, B_{max} is the amount of hydrogen adsorbed at the saturation point, and α and n are isotherm parameters. The extrapolated amount B_{max} represents the ultimate hydrogen uptake at the infinite pressure and 77 K.

$$B = B_{max}\frac{\alpha P^n}{1+\alpha P^n} \quad (1)$$

2.2. Calculation of descriptors

Most descriptors including electrotopology and polar surface area (PSA) were calculated with the program package QSAR [19] in Materials Studio (version 3.2) of Accelrys Inc. [26]. The electrotopological state indices for a particular atom resulted from the topological and electronic environment. These indices

Table 1
Hydrogen uptakes of various MOFs

Structures	Final uptake (FU) (wt%, 1 atm)	Ultimate uptake (UU) (wt%, ∞ atm)	Relative uptake (RU = UU/FU)	Mean second order derivative		
				0.00–0.50 (atm)	0.25–0.75 (atm)	0.50–1.00 (atm)
IRMOF-1[a,b]	1.31	4.71	3.60	−1.96	−1.16	−0.76
IRMOF-3[a]	1.40	4.40	3.14	−3.20	−1.48	−0.88
IRMOF-8[a,b]	1.50	16.22	10.81	−5.80	−1.48	−0.72
IRMOF-11[a,b]	1.62	12.08	7.46	−4.76	−1.56	−0.80
IRMOF-18[b]	0.89	3.16	3.55	−1.24	−0.76	−0.52
IRMOF-3β[c]	1.55	5.84	3.77	−2.36	−1.32	−0.88
Nitro-MOF[c]	1.01	2.06	2.04	−2.40	−1.36	−0.80
Zn26NDC_dabco[c]	0.78	1.05	1.35	−5.40	−0.84	−0.28
Zn27NDC_block[c]	1.30	3.08	2.37	−7.84	−1.56	−0.68
ZnBTBd[c]	0.92	1.31	1.42	−6.64	−1.12	−0.44

Final uptake is the amount of adsorbed hydrogen molecules at 77 K, 1 atm, and the ultimate uptake is estimated amount after the Langmuir–Freundlich fitting. The relative uptake is a ratio of ultimate uptake to final uptake. The framework formula of each MOF is mentioned in the main text.

[a] Ref. [34].

[b] Ref. [6].

[c] This work.

encoded the electronegativity as well as the local topology of each atom by considering perturbation effects from its neighbors. The PSA was defined as the surface area occupied by the polar atoms having the absolute value of partial charge greater than 0.2*e*. The iso-value surface area of electrostatic potential (ESP) was derived separately from the Mulliken charges calculated by density functional theory (DFT) with the program package DMol^3 [27,28] in Materials Studio (version 3.2) of Accelrys Inc.

2.3. Prediction of hydrogen uptake based on regression analysis

Before the regression analysis, all the descriptors had been normalized, that is, the extensive molecular descriptors were transformed to intensive properties by dividing them with formula weights. After the calculation with Materials Studio QSAR and the analysis with the iso-value surface area of electrostatic potential, we got 204 values for the descriptors which were reduced further down to 110 values by applying the correlation matrix analysis. Because the molecular dimensions of MOFs analyzed are all different, only the intensive values were selected and extensive ones were not used. Among the reduced 110 descriptors important molecular descriptors were chosen by using the genetic algorithm, and these descriptors were used to determine the adsorption amount of hydrogen molecules. Friedman lack of fit (LOF) was used as a scoring function and scaled LOF smoothness parameter and mutation probability were set to 0.5 and 0.1, respectively. We could make equations with three terms.

Finally, three descriptors were used for the formulation of regression equation, and validation of the regression equation was performed with R^2 and Q^2 value (Table 2). R^2 was defined as the fraction of the total variance of the Y variable (experimental data) and Q^2, the cross-validated equivalent of R^2, was derived from cross-validation. The expressions of these values are

$$R^2 = \frac{\mathrm{SSR}}{\mathrm{SST}} \tag{2}$$

$$Q^2 = 1 - \frac{\mathrm{PRESS}}{\mathrm{SST}} \tag{3}$$

where SSR is the sum of squares of regression, SST is the total sum of squares, and PRESS is the predictive sum of squares of a model [29]. Each term in the resulting equations was examined to determine the factors affecting hydrogen uptake.

2.4. Classification of MOFs based on uptake pattern

For the classification of the adsorption pattern of hydrogen molecules, recursive partitioning was performed [30]. During the recursive partitioning process, models were constructed by successive splitting of a dataset into homogeneous subsets based on a set of descriptor queries. We defined the activity for the recursive partitioning as the presumed saturation amount of hydrogen and three clusters were adapted as 0, 1 and 2. The CSAR (classification structure activity relationship) module in Cerius^2 4.10 [31] was used for the recursive partitioning and the descriptors for the classification were identical with those for the genetic algorithm analysis. Advanced lookahead with 2 clusters per class and scoring splits methods were used. Gini Impurity with generality factor and limit knuts per variable were set to 0.5 and 20, respectively.

3. Results and discussion

3.1. Prediction of hydrogen uptake

The MOFs used to calculate the descriptors are listed in Table 1. The hydrogen uptakes measured at 77 K and 1 atm are represented as the final uptake (FU), and the saturation values predicted by Langmuir–Freundlich fitting are as the ultimate uptake (UU). We compared the hydrogen amount based on the relative ratio of ultimate and final hydrogen uptake, the relative uptake (RU). The relative uptake could be thought as the extent of saturation of hydrogen molecules which adsorbed into MOFs at the measurement conditions. For example, the large relative uptake value found in IRMOF-8 indicates that its pore is not used efficiently or sufficiently for the storage of hydrogen molecules at that condition. For the examination of curvature of hydrogen uptake plot (Fig. 1), mean second derivatives were calculated over the three overlapping regions from 0 to 1 atm. Rapid initial increment of hydrogen uptake at lower pressure is expected to increase the absolute value of second order derivatives.

After the genetic algorithm analysis we could identify the important variables which influence hydrogen adsorption

Table 2
Linear combination of 2D and 3D descriptors as a result of multiple linear regression

R^2	Q^2	Equation	Definition
FU			
0.91	0.79	$Y = 0.348488739 \times$ X11 + 0.000767785 × X15 + 0.023889971 × X48 − 0.02134	X11: specific[a] ESP(+0.009); X15: molecular refractivity; X48: dipole moment
UU			
0.89	0.74	$Y = 3.115897843 \times$ X4 + 0.009243973 × X15 + 22.287571606 × X30 − 39.901306667	X4: specific[a] ESP(−0.005); X15: molecular refractivity; X30: molecular shadow area fraction^{-1}
RU			
0.86	0.62	$Y = 2.065034894 \times$ X4 + 0.005460121 × X15 + 12.766121949 × X30 − 22.387596901	X4: specific[a] ESP(-0.005); X15: molecular refractivity; X30: molecular shadow area fraction^{-1}

[a] "Specific" means the value was normalized by the weight for the conversion of extensive value to intensive one.

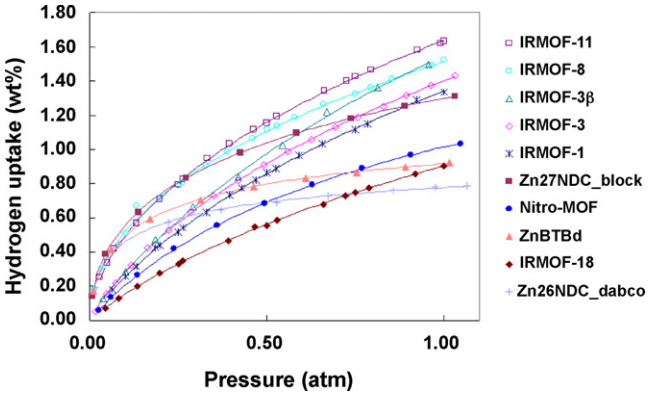

Fig. 1. Hydrogen uptake plots. The solid lines are the result of Langmuir–Freundlich fitting.

capability of MOFs. Two major descriptors, electrostatic potential and polar surface area, and the iso-value surface area of electrostatic potential are summarized in Fig. 2 and Table 2, respectively.

We compared the observed hydrogen uptake with the calculated value; the FUs are shown in Fig. 3, the UUs in Fig. 4, and the RUs in Fig. 5, respectively. These results show that the correlation between the observed and calculated hydrogen uptakes is acceptable though the number of experimental values is not sufficiently large. However, the limitation of the fitting method may cause incorrect UU prediction.

The RUs have been represented as the equations of multiple linear regressions in Table 2. We included molecular shadow area fraction as a descriptor in the regression. It can be obtained by projecting molecular or framework structure to any crystallographic planes which means the windows of MOFs for the penetration of hydrogen molecules, and it shows up in the regression equations of ultimate and relative uptake. Thus, as the pressure increases and the hydrogen uptake proceeds more and more in MOFs, the window size becomes an important factor determining the increment of hydrogen uptakes.

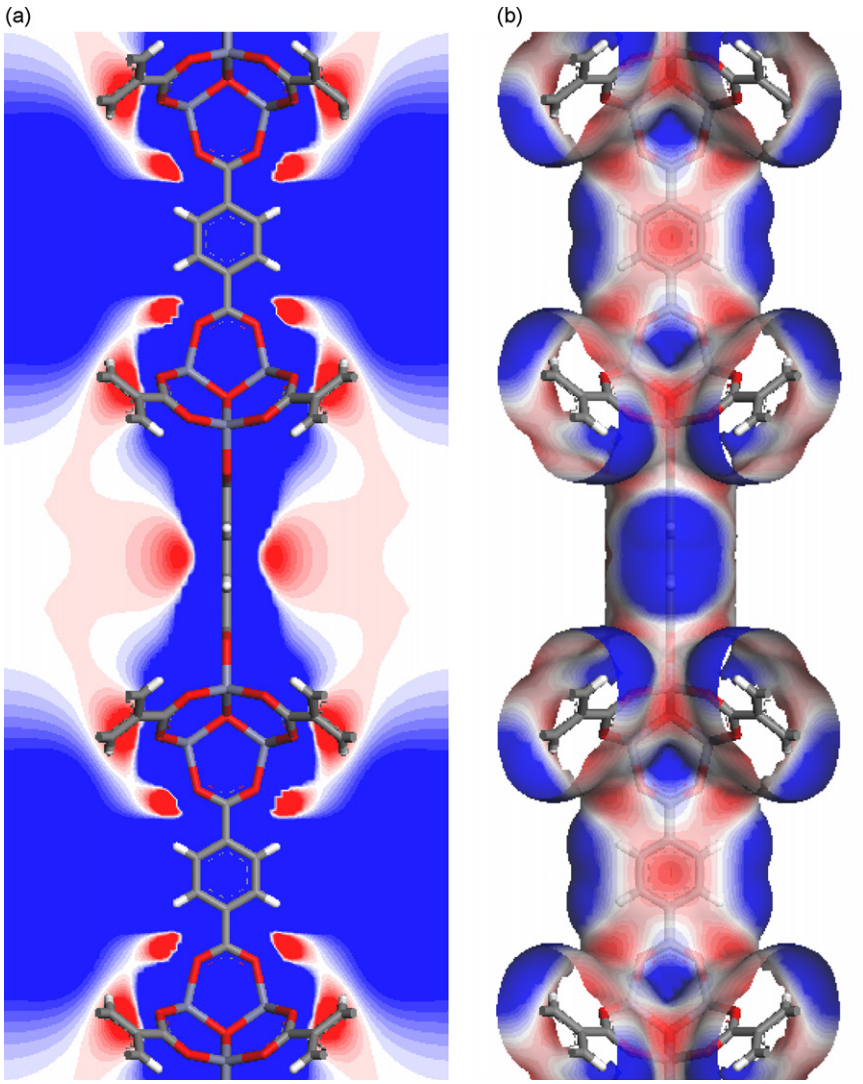

Fig. 2. Molecular surface areas. Nucleophilic region is shown in red and electrophilic region is shown in blue. (a) Contour map of electrostatic potential. (b) Accessible surface area which contains the electrostatic potential.

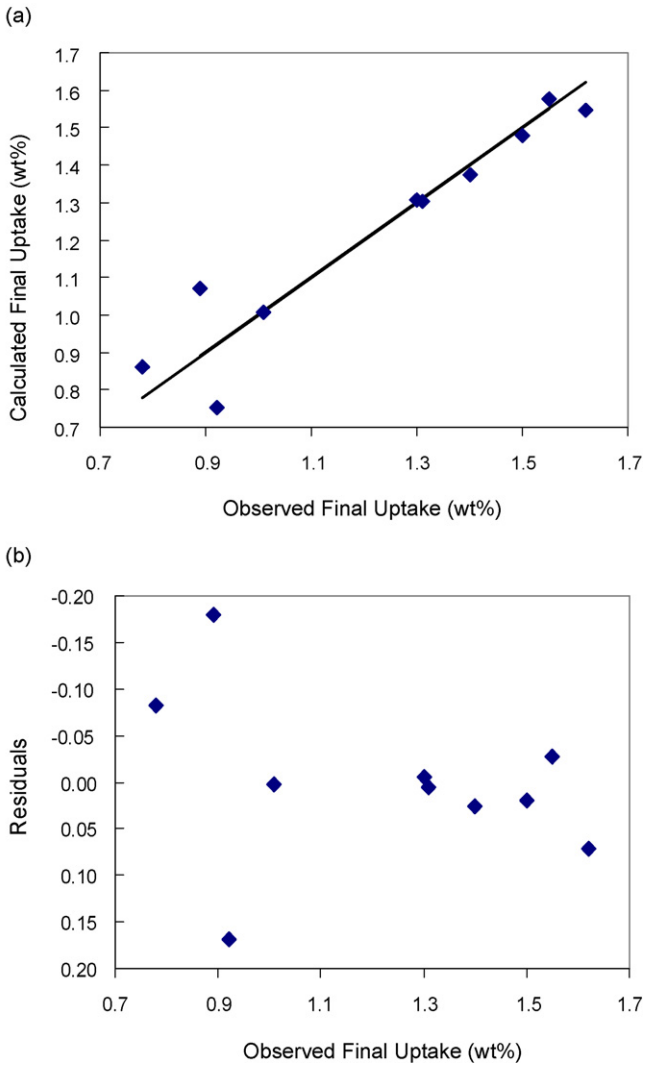

Fig. 3. Multiple linear regression model for the prediction of final hydrogen uptake using a linear combination of 2D and 3D descriptors. (a) The hydrogen uptake estimated from the combined 2D and 3D matrix. (b) Differences between the calculated and observed hydrogen uptakes.

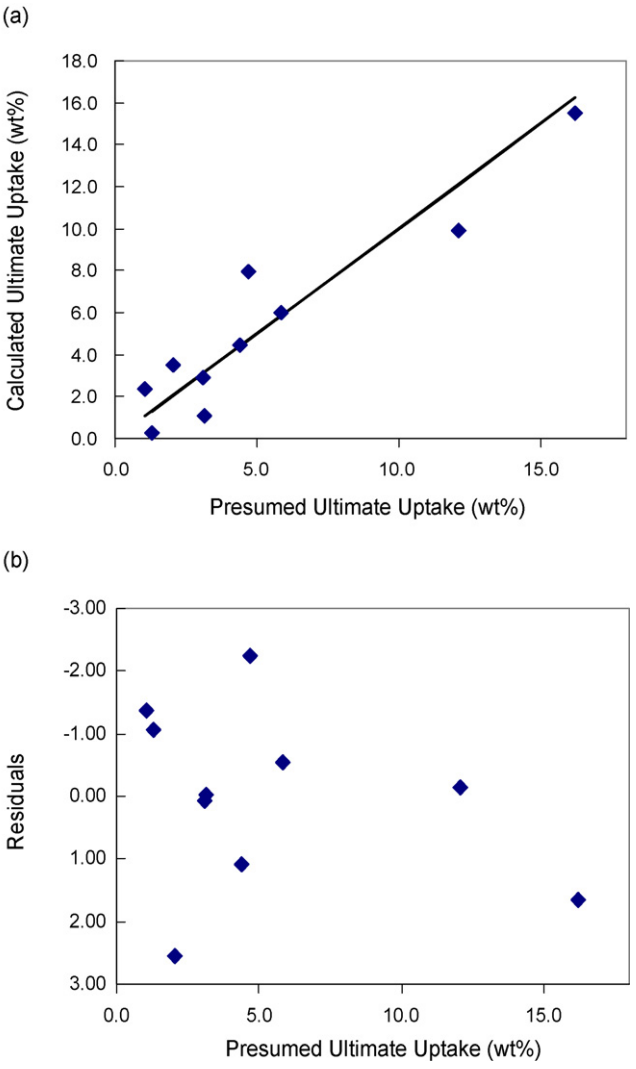

Fig. 4. Multiple linear regression model for the prediction of ultimate (saturated) hydrogen uptake using a linear combination of 2D and 3D descriptors. (a) The hydrogen uptake estimated from the combined 2D and 3D matrix. (b) Differences between the calculated and observed hydrogen uptakes.

3.2. Recursive partitioning

We also performed the recursive partitioning based on ultimate uptake values that presume the saturation of hydrogen adsorption. 10 MOFs studied are divided into three classes as shown in Fig. 6; IRMOF-1, IRMOF-3, IRMOF-18, IRMOF-3β and Zn27NDC belong to class 1, IRMOF-8 and IRMOF-11 to class 2, and Nitro-MOF, Zn26NDC_dabco and ZnBTBd to class 3. FNSA3 and molecular shadow area fraction were used as descriptors for the classification. The Jurs descriptor FNSA3 is fractional atomic charge-weighted negative surface area, which is the atomic charge-weighted negative surface area divided by the total molecular solvent-accessible area [32]. Molecular shape area fraction is one of the spatial descriptors and represents the fractional area of molecular shadow in a rectangular plane [33]. In the classification flow chart of Fig. 6, the first node is branched off according to the relative ratio between polar surface area and total accessible surface area. The remaining five MOFs were divided into two classes at the second node according to the molecular shadow area ratio which is the window of frameworks for the hydrogen molecules. These results showed that the polarization and the window size in the frameworks of MOFs could be the key factors representing the properties of the hydrogen adsorption into MOFs.

At the low temperature, 77 K, the interaction between hydrogen molecules and MOFs is closely related with the electrostatic potential given by the frameworks of MOFs. So both the iso-value surface area of electrostatic potential energy and the polar surface area have correlations with hydrogen uptake, which has been supported by the theoretical calculation [18]. Sufficient polar surface area provides potential sites for hydrogen adsorptions close to the adsorbent, and electrostatic potential energy shows that hydrogen molecules can be adsorbed in multiple layers. At higher temperature, however, the main interaction may not originate from electrostatic

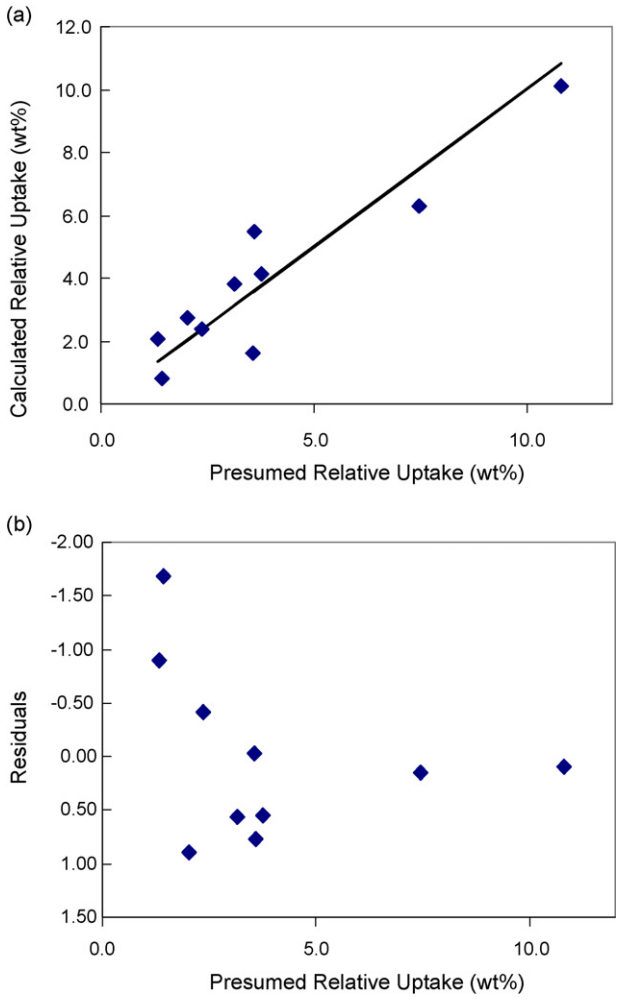

Fig. 5. Multiple linear regression model for the prediction of relative ratio of ultimate and final hydrogen uptake using a linear combination of 2D and 3D descriptors. (a) The hydrogen uptake estimated from the combined 2D and 3D matrix. (b) Differences between the calculated and observed hydrogen uptakes.

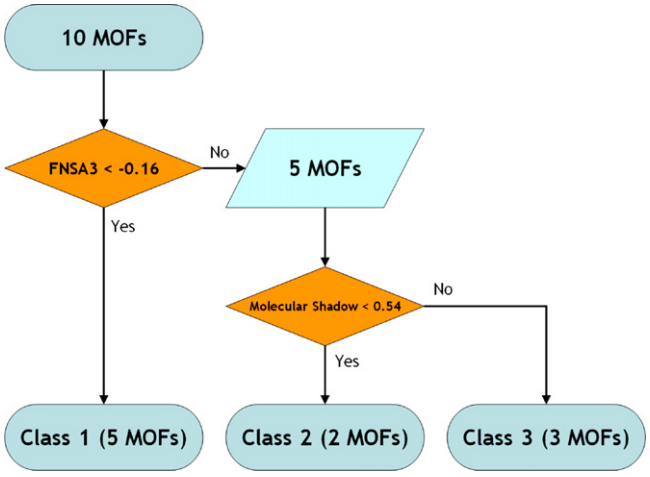

Fig. 6. Classification of hydrogen uptakes as a result of recursive partitioning. IRMOF-1, IRMOF-3, IRMOF-18, IRMOF-3β and Zn27NDC_block belong to class 1, IRMOF-8 and IRMOF-11 to class 2, and Nitro-MOF, Zn26NDC_dabco and ZnBTBd to class 3.

potential and more careful consideration is necessary to find out optimal adsorption conditions. For example, the entropic contribution to the interaction becomes more important than the binding enthalpy at room temperature. Unfortunately hydrogen sorption data at room temperature are very limited currently making QSPR studies at higher temperature difficult.

4. Conclusions

We have evaluated several quantitative factors as potential parameters to correlate molecular structures of MOFs with their hydrogen sorption properties. For the 10 MOFs analyzed in this study, we could find good correlation between the observed and calculated values of hydrogen uptake. Three structural descriptors developed during this quantitative structure–uptake relationship analysis may be successively used to predict the amount of hydrogen uptake of other MOFs.

The electron delocalization and polarization of the organic linker in the frameworks were correlated with the interaction strength of the framework with hydrogen molecules adsorbed. In addition, the electrostatic potential surface of the MOFs could provide information on the interaction modes between the framework and hydrogen molecules. It was also found that the framework window becomes another important factor for hydrogen adsorption and desorption if the hydrogen density in MOFs gets increased.

Acknowledgements

This research was performed for the Hydrogen Energy R&D Center, one of the 21st Century Frontier R&D Program, funded by the Ministry of Science and Technology of Korea. We thank Accelrys Korea for the support of modeling software.

References

[1] S. Kitagawa, R. Kitaura, S. Noro, Angew. Chem. Int. Ed. 43 (2004) 2334.
[2] N.L. Rosi, J. Eckert, M. Eddaoudi, D.T. Vodak, J. Kim, M. O'Keeffe, O.M. Yaghi, Science 300 (2003) 1127.
[3] J.L.C. Rowsell, O.M. Yaghi, Angew. Chem. Int. Ed. 44 (2005) 4670.
[4] E.Y. Lee, M.P. Suh, Angew. Chem. Int. Ed. 43 (2004) 2798.
[5] D.N. Dybtsev, H. Chun, K. Kim, Angew. Chem. Int. Ed. 43 (2004) 5033.
[6] J.L.C. Rowsell, A.R. Millward, K.S. Park, O.M. Yaghi, J. Am. Chem. Soc. 126 (2004) 5666.
[7] B. Kesanil, Y. Cui, M.R. Smith, E.W. Bittner, B.C. Bockrath, W. Lin, Angew. Chem. Int. Ed. 44 (2005) 72.
[8] Y. Kubota, M. Takata, R. Matsuda, R. Kitaura, S. Kitagawa, K. Kato, M. Sakata, T.C. Kobayashi, Angew. Chem. Int. Ed. 44 (2005) 920.
[9] G. Férey, M. Latroche, C. Serre, F. Millange, T. Loiseau, A. Percheron-Guégan, Chem. Commun. 24 (2003) 2976.
[10] D.N. Dybtsev, H. Chun, S.H. Yoon, D. Kim, K. Kim, J. Am. Chem. Soc. 126 (2004) 32.
[11] L. Pan, M.B. Sander, X. Huang, J. Li, M. Smith, E. Bittner, B. Bockrath, J.K. Johnson, J. Am. Chem. Soc. 126 (2004) 1308.
[12] A.M. Seayad, D.M. Antonelli, Adv. Mater. 16 (2004) 765.
[13] Y. Okamoto, Y. Miyamoto, J. Phys. Chem. B 105 (2001) 3470.
[14] T. Mueller, G. Ceder, J. Phys. Chem. B 109 (2005) 17974.
[15] O. Hübner, A. Glöss, M. Fitchtner, W. Klopper, J. Phys. Chem. A 108 (2004) 3019.
[16] S. Hamel, M. Cô té, J. Chem. Phys. 121 (2004) 22.
[17] T. Sagara, J. Klassen, E.J. Ganz, Chem. Phys. 121 (2004) 12543.

[18] D. Kim, T.B. Lee, S.B. Choi, J.H. Yoon, J. Kim, S.-H. Choi, Chem. Phys. Lett. 420 (2006) 256.
[19] D. Rogers, A.J. Hopfinger, J. Chem. Inf. Comp. Sci. 34 (1994) 854.
[20] L. Breiman, J.H. Friedman, R.A. Olshen, C.J. Stone, Wadsworth (1984).
[21] D.M. Hawkins, S.S. Young, A. Rusinko III, Quant. Struct. Act. Relat. 16 (1997) 296.
[22] A.M. Van Rhee, J. Stocker, D. Printzenhoff, C. Creech, P.K. Wagoner, K.L. Spear, J. Comb. Chem. 3 (2000) 267.
[23] P.D. Mosier, P.C. Jurs, J. Chem. Inf. Comput. Sci. 42 (2002) 1460.
[24] R.T. Yang, Gas Separation by Adsorption Processes, Butterworth, Boston, 1997.
[25] (a) S.S. Kaye, J.R. Long, J. Am. Chem. Soc. 127 (2005) 6506;
(b) B.U. Choi, D.K. Choi, Y.W. Lee, B.K. Lee, J. Chem. Eng. Data 48 (2003) 603;
(c) J.G. Jee, M.K. Park, H.K. Yoo, K. Lee, C.H. Lee, Sep. Sci. Technol. 37 (2002) 3465;
(d) J. Yang, S. Han, C. Cho, C.H. Lee, H. Lee, Sep. Technol. 5 (1995) 239.
[26] Accelrys, MS Modeling Release 3.2, Accelrys Software Inc., San Diego, 2005.
[27] B. Delley, J. Chem. Phys. 92 (1990) 508.
[28] B. Delley, J. Chem. Phys. 113 (2000) 7756.
[29] B.F. Manly, Multivariate Statistical Methods: A Primer, Chapman and Hall, London, 1986.
[30] A.M. van Rhee, J. Stocker, D. Printzenhoff, C. Creech, P.K. Wagoner, K.L. Spear, J. Comb. Chem. 3 (2000) 267.
[31] Accelrys Software Inc., Cerius2 Release 4.10, Accelrys Software Inc., San Diego, 2005.
[32] D. Stanton, P. Jurs, Anal. Chem. 62 (1990) 2323.
[33] R.H. Rohrbaugh, P.C. Jurs, Anal. Chim. Acta 199 (1987) 99.
[34] M. Eddaoudi, J. Kim, N. Rosi, D. Vodak, J. Wachter, M. O'Keeffe, O.M. Yaghi, Science 295 (2002) 469.